Phase Behavior of Anionic Polyelectrolyte Mixtures in Aqueous Solution. Effects of Molecular Weights, Polymer Charge Density, and Ionic Strength of Solution

Stig Hellebust,*,† Svante Nilsson,‡ and Anne Marit Blokhus†

Department Physical Chemistry, University of Bergen, Allégaten 41, N-5007 Bergen, Norway, and Institute for Surface Chemistry, Box 5607, SE-114 86 Stockholm, Sweden

Received September 6, 2002; Revised Manuscript Received May 1, 2003

ABSTRACT: Interactions between poly(sodium styrenesulfonate) (NaPSS) and sodium polyacrylate−acrylamide copolymers, NaP(AA/AM), in aqueous solutions have been studied. Equilibrium pseudoternary phase diagrams have been determined, for varying combinations of molecular weights and charge densities of the components and with varying concentrations of salt in solution. All the fully charged mixtures segregate at sufficiently high concentrations of polyelectrolytes (typically 6−8 wt %). Addition of salt and/or increasing the molecular weight results in a larger two-phase area in the diagrams. The main finding on reducing the charge density of one of the components P(AA/AM) is that the extent of the two-phase region changes relatively little until the charge density is reduced to about 20%, where, abruptly, complete miscibility occurs. The phase behavior is qualitatively reproduced by a modified Flory−Huggins model where dissociated counterions are included as a separate component contributing to the entropy of mixing. Experimental observations and theoretical modeling suggest that the model presented is a promising tool for achieving better quantitative, as well as qualitative, predictions of phase behavior of polyelectrolyte−polyelectrolyte−solvent systems, if appropriate modifications are implemented.

Introduction

Phase separation is a common feature of mixed polymer solutions. Various applications exploit the tendency toward phase separation in polymer mixtures, such as aqueous two-phase partitioning of biological macromolecules.[1,2] But whether phase separation is desired or not, it is important to understand the underlying mechanisms or molecular interactions governing the phase behavior of a given system, for practical applications.

Despite the considerable amount of research in the field of segregating polymer mixtures, the molecular interactions in the systems are inadequately understood, but theoretical models have been proposed.[3−14] The majority of systems studied have consisted of mixtures of nonionic macromolecules.[2] The better the interactions that govern polymer mixing in water are understood, the better one is able to control practical separation processes. There have, as of yet, been comparatively few studies on phase separation in mixtures of similarly charged polyelectrolytes.[15,16] Such systems may have advantages over uncharged systems in the separation of proteins due to the tunable charge in the system arising from the dissociated counterions of the polyelectrolytes.[15,17]

Studies have been carried out on the phase behavior in aqueous mixtures of nonionic polymers,[1] nonionic polymers and polyelectrolytes,[10,18,19] oppositely charged macromolecules,[20−22] and mixtures of polymers or polyelectrolytes and surfactant micelles.[20,23−27] A review is presented in ref 28. For example, it has been found that segregating mixtures of nonionic polymers can be made completely miscible if one introduces charges on one of the components.[15,29] This has been attributed to the effect of the dissociated counterions. It is entropically unfavorable to isolate the counterions in one of the phases, and they will disperse in both phases. Since each phase must be electrically neutral, the polyions partition into both phases. The result is enhanced miscibility. This type of miscibility is entropy driven.[30] However, if the solvent contains salt, there will be an abundance of co-ions in solution to fulfill the electroneutrality requirement, and the macromolecules can segregate into separate phases[15] with little entropy loss.

By making appropriate selection of water soluble polymers and ionic strengths, one can achieve ternary systems with phase behavior ranging from segregation at low concentrations to total miscibility as well as associative separation.[15] By segregative separation is understood the formation of two polymer rich phases in equilibrium, where each polymer is enriched in separate phases. The term associative separation, on the other hand, suggests that both polymers are concentrated in the same phase in equilibrium with a dilute phase consisting of mostly solvent. Furthermore, when one or both of the polymers contain charges on the chain, there exists a possibility of ”tuning” the phase behavior of the system by adjusting the interactions between the components,[15,17] for example, by altering the pH, charge density, or ionic strength.

The phase behavior of aqueous mixtures of the polyelectrolytes poly(styrenesulfonate) sodium salt and poly(acrylic acid-*co*-acrylamide) sodium salt was investigated, and the effects of varying degrees of polymerization of the components, ionic strengths of solution, and acrylamide content, that is, charge density, on the poly(acrylic acid-*co*-acrylamide) chain were observed. The segregating polyelectrolyte mixture of poly(styrenesulfonate) (PSS) and poly(acrylic acid) (PAA) that was studied here has also been studied by Bergfeldt et al.,[16] but with other permutations of molecular weights of the components. However, when varying the charge density

---

[†] University of Bergen.

[‡] Institute for Surface Chemistry.

* Corresponding author.

10.1021/ma021442t CCC: $25.00

Table 1. Molecular Weight Averages from SEC Measurements and Manufacturers' Values

polymer	wt avg MW (M_w)	number avg MW (M_n)	M_w/M_n (PDI)	repeating units^a (from M_n)
PSS500	500 000^b	166 667	3^b	800
PSS1000	1 128 000^c	238 000^c	4.7	1150
PAA225	225 000^b		3^d	800
PAA450	450 000^b	112 500	4^b	1560

[a] Repeating units are calculated from number average molecular weights using monomer formula weights. [b] Manufacturer's value. [c] Measured value. [d] Assuming the value is in the normal range.

of PAA by changing its neutralization degree, they found what was termed an S−A transition, whereby the pair segregated at high degrees of neutralization, α, of PAA and associated at low α. In this study the charge density was varied by changing the percentage of carboxylic groups on a poly(acrylamide) chain and ensuring that all acid groups were ionized by addition of NaOH. Using a poly(acrylamide) backbone removed the tendency for association at low charge densities. Thus, the effect of charge density in a purely segregative system could be investigated.

A model based on Flory−Huggins theory, modified to take into account the entropy of mixing of the dissociated counterions, has been tested against experiment.

Experimental Section

Materials. Poly(acrylic acid) sodium salt of molecular weight 225 000 Da (PAA225) was purchased from Polysciences, Inc. as solution of 20 wt % of solids in water and used without further purification. Poly(acrylic acid) of molecular weight 450 000 Da (PAA450) was purchased from Scientific Polymer Products, Inc. and dissolved in water. Polystyrenesulfonate sodium salt of molecular weight 1 000 000 Da was obtained from Aldrich. Polystyrenesulfonate sodium salt of molecular weight 500 000 Da (PSS500) was obtained from Scientific Polymer Products, Inc. The latter contained some insoluble materials that were removed by centrifugation. The pH was adjusted with NaOH(s) to a value of 10 or higher in all samples, to ensure complete dissociation of the carboxyl groups on the PAA chain in solution.[31] For the polyacid, this ensured that the charge density, α, was maintained at or near unity. PSS is a strong electrolyte and will be fully dissociated.

Polydispersity indices, defined as the ratio of weight average molecular weight over number average molecular weight, $\overline{M_w}/\overline{M_n}$, for PSS500 and PSS1000, were measured with size exclusion chromatography (SEC) with a column set of Waters Ultrahydrogel 2000 (pore size 2000 Å), Waters Ultrahydrogel 1000 (pore size 1000 Å), and Waters Ultrahydrogel Linear (mixed bed) columns, connected to a UV detector. The values measured were within the normal range for commercially available polymers. Polydispersity indices are given in Table 1. The polydispersity index for PAA225 was not measured and was not available from the manufacturer, but a value of 3 was assumed when calculating number average molecular weight that was needed for the modeling. A value lower than 3 is unrealistic.

Poly(acrylamide-*co*-acrylic acid) copolymers (PAM-τ, where τ denotes degree of hydrolysis) had molecular weight 200 000 Da and were purchased from Polysciences Inc. (τ equal to 10 and 70%) and Aldrich (τ equal to 20 and 80%). Potentiometric titration[32] of these components showed the degree of hydrolysis to be 60 and 70% for the PAM-70 and PAM-80, respectively, and the nominal values for PAM-10 and PAM-20. Because of the need to ensure full ionization of the acrylate units in solution, the pH was adjusted with addition of NaOH. This can lead to hydrolysis of acrylamide groups on the polymer backbone during equilibration of samples. To determine the extent of this autohydrolysis, a solution of PAM200(20) was prepared as for the segregating samples, but without the PSS component. Aliquots were taken and analyzed on consecutive days to see if the degree of hydrolysis increased. It was found that it was increased by about 12% the first day and about 13% after 4 days. Thus, all samples were prepared, equilibrated, and separated within a period of 4 days to ensure that the observed effects were not due to uncontrolled autohydrolysis in the samples. The component with a nominal value of 20% hydrolysis on the polymer chain was therefore in reality closer to 30% hydrolyzed. The autohydrolysis of the copolymers with higher charge densities was checked and found negligible within the experimental time frame.

Phase Diagrams. Pseudoternary phase diagrams were determined by the tie-line method. The coexistence curve was drawn through the end points of the tie lines determined for the system.

Samples of appropriate concentrations of polyelectrolytes were prepared and stored at 25 ± 1 °C until phase separation was achieved, whereupon samples were centrifuged at 2600 rpm for 1−3 h. After centrifugation, the separated phases were collected separately and analyzed. The PSS concentration in the PSS−PAA systems was determined by UV spectroscopy at 249 and 261 nm and was calculated from a double calibration to minimize the influence of the PAA component. The analytical value was within an interval ±0.5 wt % around the real value estimated from analyses on test solutions. For the PSS−PAM-τ samples ($\tau < 100\%$), PSS was determined from a partial least squares regression[33] model based on the UV absorbance spectra for wavelengths between 248 and 280 nm or by the method described above.

The concentration of PAA or PAM-τ was determined by refractive index measurements taking into account the contributions from the previously determined PSS concentration and the salt and NaOH concentrations determined analytically. The contribution from each of the four constituents was determined by multiple linear regression on a set of calibration samples. The experimental error for PAM-τ determination was mostly influenced by the uncertainty in PSS and NaOH concentrations and found to lie within the interval ±0.5 wt % around the real value. For our purpose, this is an acceptable degree of accuracy.

For some systems (see Results and Discussion section), the coexistence curves were also determined by the cloud point method on separate samples, at 25 ± 1 °C. For this method, stock solutions of the polyelectrolytes of suitable concentration (wt/wt) were prepared in pure water or aqueous NaCl solution of appropriate concentration. For each system, several phase separated samples were obtained by mixing the appropriate stock solutions, and the samples were diluted with the appropriate solvent until the one phase region was reached. For mixtures in pure water this was determined as the concentration where no turbidity was visible upon standing for several days in a thermostated bath. For samples dissolved in aqueous NaCl solution, the one phase region was recognized when no phase separation could be observed. For these samples the interface between the separated phases was clearly visible until a sharp transition to clear mixtures on further addition of solvent was observed, whereas for salt free mixtures the transition was one from a turbid mixture to a clear one. However, for the systems containing PAM-60 and PAM-70 this method was not applicable because of inherent turbidity in stock solutions, so the change in turbidity of the mixture could not be used as a criterion for transition. It was still possible to observe whether the sample had segregated in two phases, but the coexistence curves for these systems were determined by the tie-line method.

A mass balance check of the separated phases was carried out after determination of the compositions in each phase. The averages of the residuals between the estimated total concentrations of the respective polymers, based on analyses and phase volumes, and the concentrations as prepared were close to zero with standard deviations of 0.7% and 0.5% for PAA and PSS, respectively.

Salt and Sodium Concentrations. The sodium chloride concentration of each phase, if present, was determined in most of the segregated samples, by titration with an acidic solution of $Hg(NO)_3$ from Merck and a 2% solution of diphenylcarbazone from Fluka in 95% ethanol as indicator.[34] The accuracy and precision of this method were found to be very satisfactory. Sodium ion concentrations were analyzed on a Corning clinical Flame Photometer 410c with a propane flame.

Theoretical Model

The Flory−Huggins theory[6] is a lattice mean-field approximation to macromolecular solutions. It considers that there is an entropy of mixing contribution and an interaction energy contribution to the Gibbs free energy of mixing, and miscibility results when this has a negative value. The entropy of mixing contribution arises from the number of possible configurations of the solutes in solution. The larger the solute, the smaller its contribution to the entropy of mixing. The interaction energy contribution arises from the interactions between the monomer units on the different macromolecules and between the monomer units and solvent molecules.[6,35]

The theoretical model used to describe the pseudoternary phase diagrams is based on the Flory−Huggins theory. Traditionally the Flory−Huggins model is applied to nonionic systems. For a nonionic system with two polymers in a common solvent, the Flory−Huggins expression for the free energy is given by[6]

$$G_{\mathrm{mix}}/kT = N_{\mathrm{tot}}(\phi_1 \ln \phi_1 + (\phi_2/M_2) \ln \phi_2 + (\phi_3/M_3) \ln \phi_3 + \chi_{12}\phi_1\phi_2 + \chi_{13}\phi_1\phi_3 + \chi_{23}\phi_2\phi_3) \quad (1)$$

where G is the Gibbs free energy of mixing, ϕ_i are the volume, or molar, fractions of each component (index 1 = solvent, index 2 = polymer 2, index 3 = polymer 3), N_{tot} is the total number of lattice sites, M_i are the number of monomer units on the polymer chains, and χ_{ii} and χ_{ij} are the binary Flory interaction parameters, which are used as fitting parameters in the model. They will not be discussed in detail in this paper, but suffice it to say that for repulsive interactions, which are most common, the value of χ is positive and for attractive interactions it would be negative. In this study, index 1 is the solvent, polymer 2 is PSS, and polymer 3 is PAA or PAM(τ).

The adaptation to ionic polymers in the model employed in this work is made by treating the counterions as an explicit component. A description of the model with calculated examples has been presented in refs 10−12. This adaptation differs from a previous extension of the Flory−Huggins therory[9] where the ions are dealt with by introducing an effective molecular weight. The counterions[9] were assumed to reduce the effective molecular weight of the polymer. In the present treatment the ions are described as an explicit component. It is further assumed that the only contribution from the ions to the free energy is the entropy of mixing.

$$G_{\mathrm{mix}} = kTN_{\mathrm{tot}}(\phi_1 \ln \phi_1 + (\phi_2/M_2) \ln \phi_2 + (\phi_3/M_3) \ln \phi_3 + \phi_4 \ln \phi_4 + \chi_{12}\phi_1\phi_2 + \chi_{13}\phi_1\phi_3 + \chi_{23}\phi_2\phi_3) \quad (2)$$

where index 4 denotes the counterions. Extending the calculations to include salt is simple in principle but has been found to lead to numerical problems. In principle, one may also have interactions between the ions and the other components described by the free energy terms $\chi_{14}\phi_1\phi_4$, $\chi_{24}\phi_2\phi_4$, and $\chi_{34}\phi_3\phi_4$. It is here assumed for simplicity that these terms are of less importance than the entropy contribution. That is, it is assumed that all interaction terms between ions and other components are equal to zero,

$$\chi_{14} = \chi_{24} = \chi_{34} = 0$$

This can be justified since the ionic content is high (at least 1 M), which entails significant electrostatic screening. Furthermore, the tie lines connect points with very similar ionic concentrations, which gives a cancellation effect between the phases for free energy terms that depend on the ionic composition.

One may also have long-range electrostatic interactions, which have been neglected here on the justification that they are screened due to the high ionic strength in the systems. For a 10 wt % solution of PAA, the counterion concentration is about 1 M. The expressions for the chemical potentials, obtained by derivation of the free energy in the usual manner, are

$$\mu_1 - \mu_1{}^\circ = kT[\ln(\phi_1) + (1 - 1/M_2)\phi_2 + (1 - 1/M_3)\phi_3 + \chi_{12}\phi_2(1 - \phi_1) + \chi_{13}\phi_3(1 - \phi_3) - \chi_{23}\phi_2\phi_3] \quad (3a)$$

$$\mu_2 - \mu_2{}^\circ = kT[\ln(\phi_2) + (1 - M_2)\phi_1 + (1 - M_2)\phi_4 + (1 - M_2/M_3)\phi_3 + M_2(\chi_{12}\phi_1(1 - \phi_2) - \chi_{13}\phi_1\phi_3 + \chi_{23}\phi_3(1 - \phi_2))] \quad (3b)$$

$$\mu_3 - \mu_3{}^\circ = kT[\ln(\phi_3) + (1 - M_3)\phi_1 + (1 - M_3)\phi_4 + (1 - M_3/M_2)\phi_2 + M_3(-\chi_{12}\phi_1\phi_2 - \chi_{13}\phi_1(1 - \phi_3) + \chi_{23}\phi_2(1 - \phi_3))] \quad (3c)$$

$$\mu_4 - \mu_4{}^\circ = kT[\ln(\phi_4) + (1 - 1/M_2)\phi_2 + (1 - 1/M_3)\phi_3 - \chi_{12}\phi_1\phi_2 - \chi_{13}\phi_1\phi_3 - \chi_{23}\phi_2\phi_3] \quad (3d)$$

It is required that the phases are electroneutral, which gives the stoichiometric condition

$$z_2L_2\phi_2 + z_3L_3\phi_3 - z_4\phi_4 = 0 \quad (4)$$

where L is the degree of ionization for the respective polymers and z is the charge number (+1 or −1).

The criterion for phase equilibrium is that the chemical potentials are equal in coexisting phases. On the basis of the degree of polymerization of the polyelectrolytes, charge density on the polyelectrolytes, chosen values of the χ parameters as fitting parameters, and arbitrarily chosen values for the chemical potential of the solvent, the model calculates phase compositions, in volume fractions, for which the chemical potentials are equal in coexisting phases. This gives a set of tie lines that combine to construct the pseudoternary phase diagram. The computational procedure is described in Appendix A.

Results and Discussion

Experimental pseudoternary phase diagrams for all the systems studied are shown in Figures 1−3. Polymer and ion concentrations in the systems shown in Figures 1 and 3 are tabulated in Appendix B. Space considerations prevent the inclusion of all samples.

The tie-line slope (STL) (average values listed in Table 2) is a useful characteristic of a system[2] and is calculated as the ratio between the concentration differences of each polymer between the phases, ΔC(PAA)/ΔC(PSS). A value of negative unity corresponds to a tie line that is parallel to the polymer 1−polymer 2 axis. For higher values (approaching zero), the tie lines are sloped away

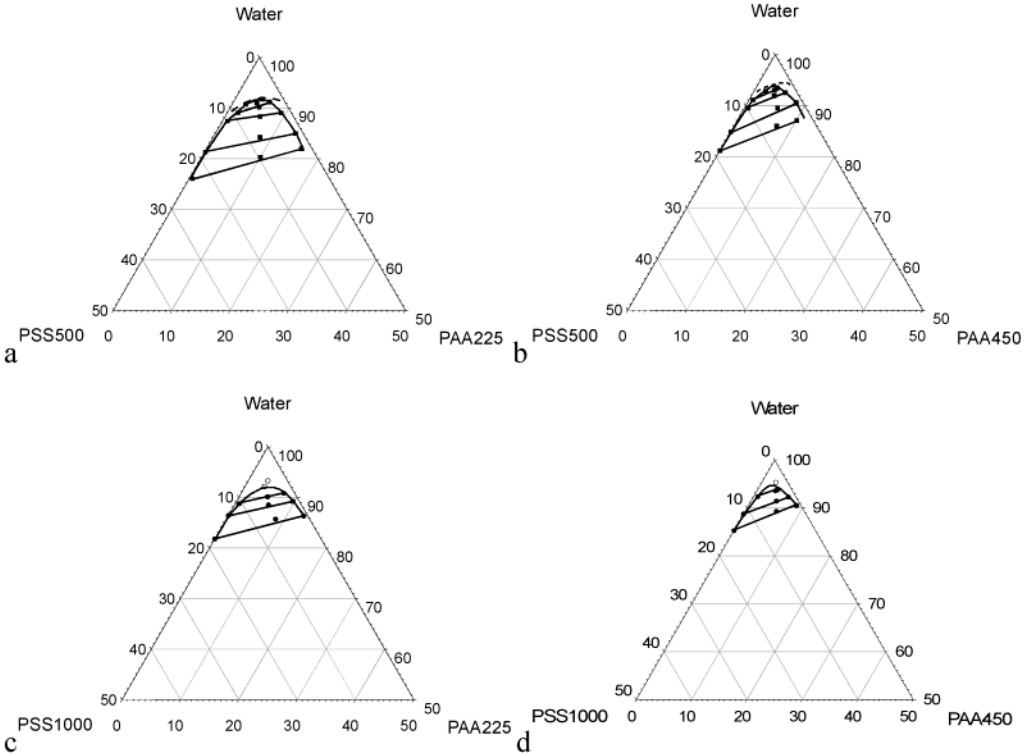

Figure 1. Pseudoternary phase diagrams at 25 °C showing the effect of increasing the molecular weight of one component, in the salt free case. Vertices are labeled with polymer type and molecular weights. Concentrations are in wt %. Filled symbols mark compositions of segregated phases and initial concentrations before segregation. Coexistence curves are drawn from cloud point determination, dashed lines (a and b), and tie-line end points, full lines (a, b, c, and d).

from the PSS component; that is, the PSS rich phase is more concentrated than the corresponding phase, as seen in all the systems presented here. A slope with zero value represents borderline separation and is neither segregative nor associative because the concentration of one of the components is exactly the same in both phases. The tie-line slopes are relatively constant within each experimental system (cf. Figures 1−3).

Influence of Molecular Weight. The pseudoternary phase diagrams of the ternary systems PSS−PAA−water are presented in Figure 1. There is a slight difference between coexistence curves determined by cloud-point and tie-line methods. This can be attributed to the effect of polydispersity in the polymer components.

In the mixture PSS500−PAA225−water, the components have a similar number of monomer units (Table 1). The coexistence curve is reasonably symmetrical with respect to the bisector of the solvent corner. In the PSS500−PAA450 mixture (Figure 1b), the PAA component has a much greater number of monomer units than PSS. The two-phase area for this system is larger. The PAA component is now much less miscible in the PSS rich phase, so the concentration difference between phases is greater. Table 2 also shows that the STL values are higher for the PSS500−PAA450 system than for the PSS500−PAA225 mixture, as one would expect, since the increased molecular weight of PAA makes it less miscible with the PSS rich phase. The critical points, which are the points where the tie-line length approaches zero, are always nearer the PSS−water axis.

When the molecular weight of PSS is increased to 1 000 000 Da (Figure 1c and d), the two-phase area does not increase much compared to those for the systems with PSS500 and the tie lines are not significantly different. However, due to the high PDI for PSS1000, the average number of monomers per chain is only about 40% greater than that for PSS500.

The tie-line slopes are comparable to those of Bergfeldt et al.,[16] who studied a system where the degree of polymerization for PSS was considerably larger than that for PAA and the observed tie lines had similar slopes to those in the PSS1000−PAA225 system in Figure 1c.

The higher the molecular weight of the components is, the lower is the concentration required for phase separation. A polymer concentration of approximately 8 wt % is required to cause phase segregation for a mixture of PSS500 and PAA225 (Figure 1a), but only about 5% total polymer is required to cause segregation for the PSS1000−PAA450 mixture (Figure 1d). Qualitatively, this is in accordance with the Flory−Huggins theory.[6]

Water distributes unevenly between the phases and leaves the PSS rich phase more concentrated; that is, the solubility of PSS in the relevant solvent is greater than the solubility of PAA in the same solvent. The PSS rich phase tends to occupy the smaller volume even if the sample had equal concentrations of each component prior to separation. The uneven distribution of water may be caused to some degree by the fact that the phases in equilibrium must have similar concentrations of charges and they are also subject to the electroneutrality condition. Thus, if each monomer unit contributes one charge, this means that, in terms of weight concentrations, the PSS rich phase must be more concentrated than the PAA rich phase, because the PSS monomers have roughly double the formula weight of the PAA monomers. For a phase consisting almost entirely of PSS to contain the same charge concentration as a phase largely consisting of PAA, the weight concentration of polyelectrolyte in the former must be

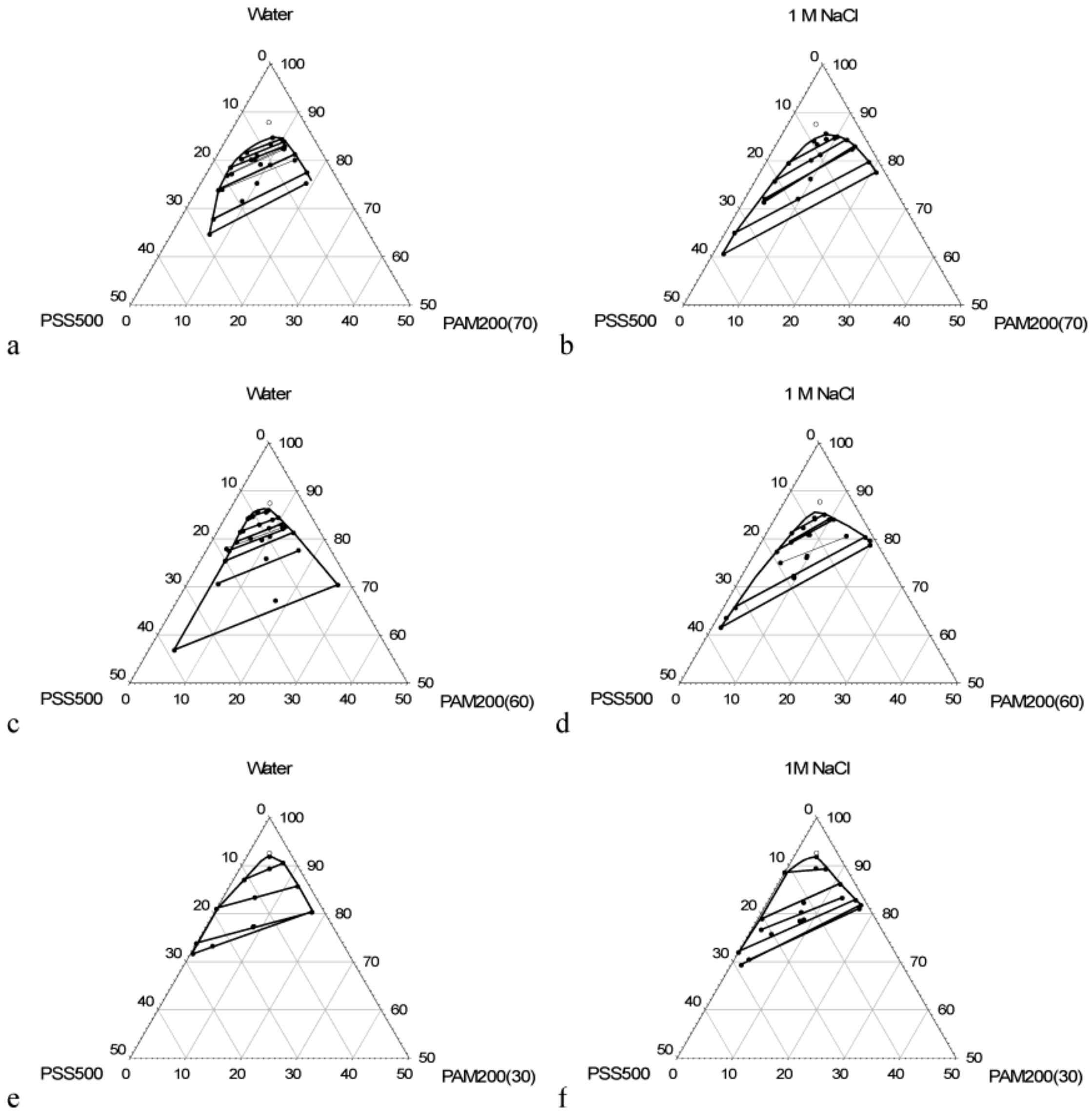

Figure 2. Pseudoternary phase diagrams at 25 °C showing the behavior of PSS500 and PAM200(τ), in water (a, c, and e) and in 1 M NaCl (b, d, and f), where τ is equal to 70% (a, b), 60% (c, d), and 30% (e, f). Vertices are labeled with polymer type and molecular weight (charge density in parentheses). Filled symbols represent compositions of segregated phases and initial compositions before segregation. Open symbols represent miscible samples. Coexistence curves are drawn from tie-line end points.

roughly double that in the coexisting phase. The observed ratio is somewhat less than 2 to 1, but there is some mixing of the components which will cause deviation from the ideal ratio.

For a mixture of nonionic polymers, the influence of molecular weight has been extensively studied. In the Flory−Huggins theory, molecular weight is taken into account only as having an influence on the entropy of mixing.[3−6] If the molecular weight of one polymer is lowered relative to that of the other component, the two-phase region shifts toward the axis of the less high molecular weight component and the coexistence curve is lowered. In a mixture of similarly charged polymers, the effect is equivalent[15] with respect to miscibility but less pronounced. The larger the difference in the molecular weights between the polymers, the more asymmetrical is the coexistence curve.[2a] The coexistence curves discussed above were not particularly asymmetrical, as Figures 1−3 show.

Influence of Charge Density. Pseudoternary phase diagrams for mixtures of copolymers of poly(acrylamide-*co*-acrylic acid) sodium salt, with varying degrees of substitution, τ, and poly(styrenesulfonate) sodium salt in water or 1 M NaCl solution are shown in Figure 2. The most striking effect of reducing charge density on one of the components is to increase the miscibility. Unlike the mixture poly(acrylic acid)−polystyrene sulfonate, which associates for low charge densities (low α) for NaPAA,[16] the mixture poly(acrylamide-*co*-acrylic acid)−polystyrenesulfonate is single phased or segregates at low charge densities (low τ).

The pair NaPSS and PAM-10 (molecular weights 500 000 and 200 000 Da, respectively) did not segregate even at high polymer concentrations, up to 40%, but at this and higher concentrations the samples were too viscous to make good observations. However, segregation could be induced in the accessible concentration range by increasing the ionic strength further. At a polymer composition of 20%, segregation was induced when increasing the salt concentration to 2.4 *m*, but for the ionic strength studied for the other systems, segregation was not observed.

A reduction of charge density from 100% ($\tau = 1$) to 70% ($\tau = 0.7$) or 60% ($\tau = 0.6$) increased the critical

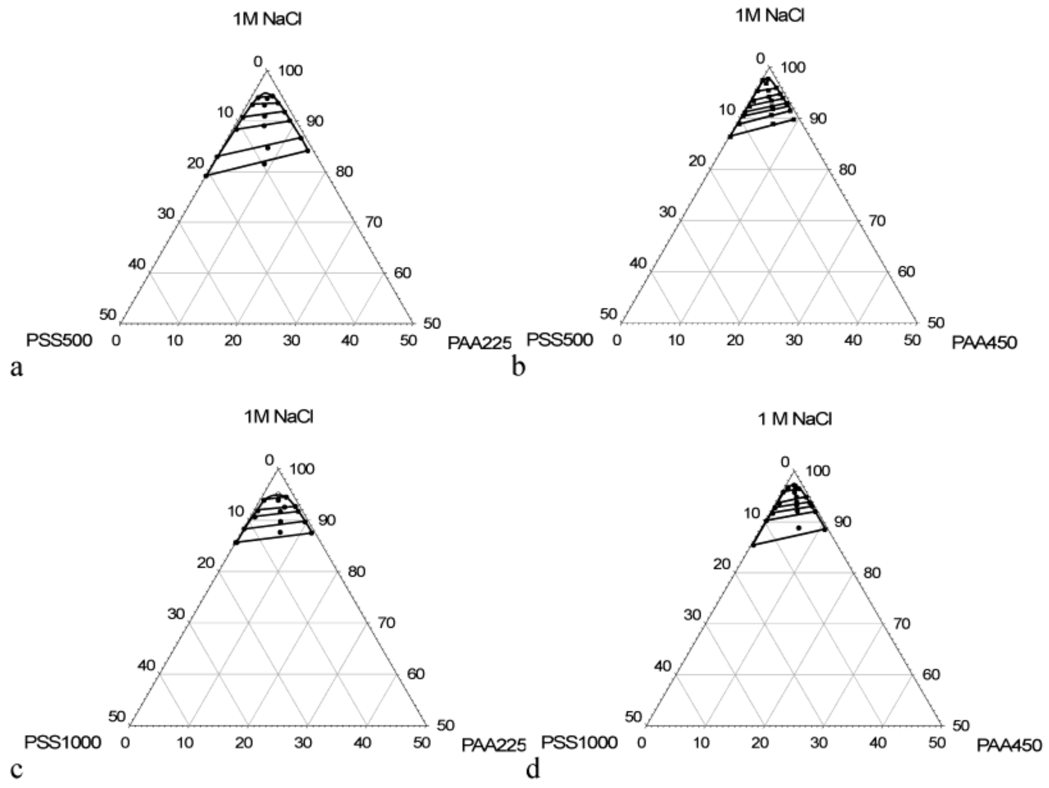

Figure 3. Pseudoternary phase diagrams at 25 °C showing the behavior of the binary mixture of fully charged polyelectrolytes in 1 M NaCl. Vertices are labeled with polymer type and molecular weights. Concentrations are in wt %. Filled symbols mark compositions of segregated phases and initial concentrations before segregation. Coexistence curves are drawn from tie-line end points.

Table 2. Average Slopes of Experimental Tie Lines

MW(PAA) (kDa)	MW(PSS) (kDa)	α(PAM)	solvent	STL[a]
225	500	100%	water	−0.74
225	500	100%	0.3 M NaCl	−0.81
225	500	100%	1 M NaCl	−0.84
450	500	100%	water	−0.60
450	500	100%	0.3 M NaCl	−0.68
450	500	100%	1 M NaCl	−0.80
225	1000	100%	water	−0.76
225	1000	100%	1 M NaCl	−0.86
450	1000	100%	water	−0.64
450	1000	100%	1 M NaCl	−0.79
200	500	30%	water	−0.70
200	500	30%	1 M NaCl	−0.57
200	500	60%	water	−0.61
200	500	60%	1 M NaCl	−0.52
200	500	70%	water	−0.59
200	500	70%	1 M NaCl	−0.51

[a] STL = ΔC(PAA)/ΔC(PSS). Average value for diagram.

Table 3. Polymeric and Ionic Compositions for the System Shown in Figure 1a

500-225-water	PAA wt %	PSS wt %	neg[a] charges (mol/kg solutn)	pos[b] charges (mol/kg solutn)
sample 1 top	2.27	7.00	0.58	0.59
sample 1 bot	4.57	3.64	0.66	0.73
sample 2 top	1.74	9.10	0.63	0.64
sample 2 bot	6.14	2.60	0.78	0.83
test 1[c] as prepared	3.98	1.19	0.48	
test 2[c] as prepared	1.08	2.09	0.22	
test 1 analytical	3.68	1.37	0.46	0.46
test 2 analytical	0.86	2.19	0.20	0.22

[a] Negative charges on dissociated polyanions, from analytical polymer composition and chloride ions from titration. [b] Sodium ions contributions from polyelectrolyte dissociation, NaCl for ionic strength adjustment, and NaOH for pH adjustment. Analyzed on flame photometry. [c] Tests 1−2 were control samples included to verify the analytical values.

polymer concentration from about 8% for the 500−225 ($\tau = 1$) system (Figure 1a) to about 14% for the latter systems, where $\tau = 0.7$ or 0.6 (Figure 2a and c). A reduction of charge density on the PAM chain also leads to a greater concentration difference between separated phases compared to the case of the fully charged systems, for both low and high ionic strengths, as seen by the tie-line slopes (Table 2).

At further reduction in the charge density to 30% ($\tau = 0.3$) (Figure 2e), for the mixture of PSS500 and PAM200(30), the coexistence curve is found to move closer to the solvent corner again and the critical concentration for segregation is about 8 wt % total polymer concentration. They are less miscible. This is confirmed by the titration method, whereby samples prepared in the two-phase area are diluted with appropriate solvent until no phase boundary is visible.

This enhanced miscibility compared to the case of the fully charged system in Figure 1a is likely to be an example of entropy driven miscibility. The PAM component has lower charge density relative to that of the PSS component and contributes less counterions to solution. The chemical potential of the solvent is to a large extent controlled by counterion concentration. It must be the same in both phases at equilibrium, so tie lines must connect points with (almost) the same counterion concentration. Because the PAM-τ chain has lower charge density, more chains are required to contribute the same amount of counterions and thus the solubility of PAM in the PSS rich phase is increased.

Influence of Ionic Strength−Equal Charge Densities. Figure 3 shows the same systems as in Figure 1, with 1 M NaCl as the solvent pseudophase. The systems in Figure 3a and b were also studied in 0.3 M

Table 4. Polymeric and Ionic Compositions for the System Shown in Figure 3a

500-225-1M	PAA wt %	PSS wt %	neg[a] charges (mol/kg solutn)	pos[b] charges (mol/kg solutn)
sample 3 top	1.17	4.20	1.26	1.22
sample 3 bot	3.49	1.56	1.38	1.42
sample 4 top	0.90	5.84	1.31	1.14
sample 4 bot	5.10	1.32	1.51	1.60
sample 5 top	0.54	8.73	1.39	1.40
sample 5 bot	7.13	1.08	1.70	1.78
sample 6 top	0.60	11.03	1.51	1.52
sample 6 bot	8.84	1.06	1.87	1.92

[a] Negative charges on dissociated polyanions, from analytical polymer composition and chloride ions from titration. [b] Sodium ions contributions from polyelectrolyte dissociation, NaCl for ionic strength adjustment, and NaOH for pH adjustment. Analyzed on flame photometry.

Table 5. Polymeric and Ionic Compositions for the System Shown in Figure 1c

1000-225-water	PAA wt %	PSS wt %	neg[a] charges (mol/kg solutn)	pos[b] charges (mol/kg solutn)
sample 7 top	0.00	13.55	0.66	0.67
sample 7 bot	9.61	1.13	1.08	1.13
sample 8 top	0.67	9.49	0.53	0.61
sample 8 bot	7.34	1.64	0.86	0.91
sample 9 top	0.00	16.34	0.79	0.76
sample 9 bot	12.94	0.63	1.41	1.39

[a] Negative charges on dissociated polyanions, from analytical polymer composition and chloride ions from titration. [b] Sodium ions contributions from polyelectrolyte dissociation, NaCl for ionic strength adjustment, and NaOH for pH adjustment. Analyzed on flame photometry.

Table 6. Polymeric and Ionic Compositions for the System Shown in Figure 3c

1000-225-1M	PAA wt %	PSS wt %	neg[a] charges (mol/kg solutn)	pos[b] charges (mol/kg solutn)
sample 10 top	0.18	14.15	1.62	1.67
sample 10 bot	11.84	0.62	2.15	2.17
sample 11 top	0.08	11.59	1.5	1.54
sample 11 bot	9.69	0.64	1.97	1.73
sample 12 top	0.33	7.75	1.38	1.37
sample 12 bot	7.47	0.77	1.75	1.34
sample 13 top	0.61	7.53	1.38	1.35
sample 13 bot	6.15	0.67	1.66	1.60

[a] Negative charges on dissociated polyanions, from analytical polymer composition and chloride ions from titration. [b] Sodium ions contributions from polyelectrolyte dissociation, NaCl for ionic strength adjustment, and NaOH for pH adjustment. Analyzed on flame photometry.

NaCl (not shown), for which the effect was similar to but slightly less pronounced than that in 1 M NaCl. The effect of higher ionic strength of the solvent is to increase the size of the two-phase area under the coexistence curve. The polymer concentration required to effect segregation in a 1 M NaCl solution is generally 2−3% (wt/wt) lower than the concentration required in the same mixture in pure water, for the PSS−PAA systems ($\tau = 1$ on both components). The difference between the two-phase area in 0.3 M NaCl and in 1 M NaCl solutions was relatively small, but a greater tendency for segregation with increasing ionic strength, at least up to a concentration of 1 M NaCl, was observed. The molality of chloride ions does not vary significantly between the separated phases. The concentrations of negative charges were calculated in each phase as moles of charged groups, including chloride ions, per weight of solvent, on the basis of analytical values of polyelectrolyte concentrations and salt concentration obtained by titration. Ionic concentrations for segregated phases of some samples are tabulated in Appendix B. Within experimental accuracy, the positive charges match the negative charges in each phase.

Table 7. Polymeric and Ionic Compositions for the System Shown in Figure 1b

500-450-water	PAA wt %	PSS wt %	neg[a] charges (mol/kg solutn)	pos[b] charges (mol/kg solutn)
sample 14 top	3.54	2.37	0.49	0.48
sample 14 bot	1.73	5.73	0.46	0.41
test 3[c] as prepared	2.21	1.04	0.28	
test 4[c] as prepared	1.24	2.01	0.23	
test 3 analytical	2.10	1.11	0.28	0.24
test 4 analytical	0.85	1.99	0.19	0.19
sample 15[d] top	0.84	3.17	0.24	0.49
sample 15[d] bot	0.80	7.10	0.43	0.34

[a] Negative charges on dissociated polyanions, from analytical polymer composition and chloride ions from titration. [b] Sodium ions contributions from polyelectrolyte dissociation, NaCl for ionic strength adjustment, and NaOH for pH adjustment. Analyzed on flame photometry. [c] Tests 3−4 were control samples included to verify the analytical values. [d] Sample was not used because the mass and charge balances indicated a faulty value.

Table 8. Polymeric and Ionic Compositions for the System Shown in Figure 3b

500-450-1M	PAA wt %	PSS wt %	neg[a] charges (mol/kg solutn)	pos[b] charges (mol/kg solutn)
sample 16 top	0.81	13.41	1.6	1.63
sample 16 bot	10.38	0.95	1.97	1.70
sample 17 top	0.78	8.50	1.4	1.44
sample 17 bot	7.28	0.61	1.67	1.49
sample 18 top	0.55	4.36	1.22	1.18
sample 18 bot	3.73	0.83	1.35	1.18
sample 19 top	1.04	5.90	1.32	1.32
sample 19 bot	5.02	0.75	1.48	1.35
sample 20 top	0.99	10.62	1.51	1.98
sample 20 bot	8.79	0.71	1.81	1.60

[a] Negative charges on dissociated polyanions, from analytical polymer composition and chloride ions from titration. [b] Sodium ions contributions from polyelectrolyte dissociation, NaCl for ionic strength adjustment, and NaOH for pH adjustment. Analyzed on flame photometry.

Table 9. Polymeric and Ionic Compositions for the System Shown in Figure 1d

1000-450-water	PAA wt %	PSS wt %	neg[a] charges (mol/kg solutn)	pos[b] charges (mol/kg solutn)
sample 21 top	0.00	14.73	0.71	0.65
sample 21 bot	8.68	0.8	0.96	0.89
sample 22 top	0.00	11.27	0.55	0.53
sample 22 bot	6.29	1.14	0.74	0.66
sample 23 top	3.63	2.59	0.51	0.41
sample 23 bot	0.76	6.88	0.41	

[a] Negative charges on dissociated polyanions, from analytical polymer composition and chloride ions from titration. [b] Sodium ions contributions from polyelectrolyte dissociation, NaCl for ionic strength adjustment, and NaOH for pH adjustment. Analyzed on flame photometry.

Addition of salt causes a shift in the STL values (Table 2). For all the fully charged systems, the effect of ionic strength is to reduce the STL value and even out the concentration differences in each phase. The tie lines are thus more parallel with the PSS−PAA axes for mixtures in 1 M NaCl than in the corresponding salt free systems. Other authors have found that salt concentration can differ between the phases in nonionic aqueous polymer mixtures,[2b,36] but the slight difference seen (Appendix B) in anionic charges between the phases is attributed to experimental inaccuracy in the determination of phase compositions.

Table 10. Polymeric and Ionic Compositions for the System Shown in Figure 3d

1000-450-1M	PAA wt %	PSS wt %	neg[a] charges (mol/kg solutn)	pos[b] charges (mol/kg solutn)
sample 24 top	0.37	14.17	1.60	1.59
sample 24 bot	10.89	0.61	2.0	1.63
sample 25 top	0.17	9.61	1.36	1.35
sample 25 bot	7.56	0.43	1.69	1.50
sample 26 top	0.53	7.79	1.34	1.33
sample 26 bot	6.45	0.43	1.59	1.38
sample 27 top	0.35	6.89	1.28	1.35
sample 27 bot	5.77	0.48	1.53	1.29
sample 28 top	0.63	5.70	1.25	1.15
sample 28 bot	4.54	0.58	1.42	1.17

[a] Negative charges on dissociated polyanions, from analytical polymer composition and chloride ions from titration. [b] Sodium ions contributions from polyelectrolyte dissociation, NaCl for ionic strength adjustment, and NaOH for pH adjustment. Analyzed by flame photometry.

Influence of Ionic Strength−Unequal Charge Densities. For the systems containing copolymers of lower charge densities than 100%, the effect of increasing ionic strength is to increase the concentration difference between the separated phases in equilibrium rather than reducing it. This is opposite to that of systems with equal charge densities on the components and is seen more clearly by the change in STL values accompanying the change in ionic strengths, as listed in Table 2, than in the figures. The effect is small but real. The volume ratio between segregated phases is affected by salt, in such a way that the PSS rich phase becomes smaller and more concentrated when salt is added.

It was noted above that the reduced number of counterions contributed from each PAM-τ chain requires that more chains partition into the PSS rich phase to balance charges from the freely moving counterions. This increases the concentration of PAM in the PSS rich phase. When salt is added to such a system, the electroneutrality condition can be met without partitioning of PAM chains into the PSS rich phase and hence the concentration difference between phases is allowed to increase, as observed in Figure 2b, d, and f. The miscibility is slightly reduced upon addition of salt because the direct coupling between polyelectrolyte concentration and ion concentration is removed. Nonetheless, the salt effect is weak compared to that observed in lowly charged systems.[29]

Ionic strength does not appear to affect the location of the critical point, that is, the point where the difference in phase composition disappears, but it increases the two-phase area for the PSS−PAM-τ systems by extending the tie lines further toward the polymer−solvent axes.

Modeled Phase Diagrams

Input and Output. The input required by the model algorithm is defined by eqs 3. It includes the number of monomer units on the chain, which is given by the number average molecular weight (Table 1), and the fraction of charged monomer units. This information defines the polymers' structural properties. The interaction forces in solution between the polymers and the solvent are defined by three parameters, χ_{12}, χ_{13}, and χ_{23}, as seen in eqs 3. The index 12 refers to solvent and polymer 2 (PSS in this study), index 13 refers to solvent and polymer 3 (PAA or PAM(τ) in this study), and index 23 refers to polymer 2 and polymer 3.

The output from the model is the molar fractions of solvent and monomers of each component in the separated (by segregation or association) phases if such a separation is predicted. In other words, it calculates the tie lines for the system and the predicted coexistence curve is drawn through the tie-line end points. Because the model is based on a lattice grid, where each monomer or solvent molecule occupies one site in the lattice, the predicted molar fractions are equal to volume fractions.

For the sake of ease of comparison between predicted and observed coexistence curves, the predicted molar (or volume) fractions are converted to weight fractions. The method of conversion will influence the selected parameters, but the direction of change will be unaffected, so the effects of linearly varying the parameters on reducing charge density can be studied.

Effects of Interaction Parameters on the Predicted Phase Diagrams. There are three adjustable parameters and a very large number of possible permutations of their values, even within a restricted range of values. It is necessary to get a clear idea of how they affect the resulting predictions, individually and together. This was achieved by systematically changing the parameters in a large set of model "experiments", and the following information was obtained.

The tie-line slopes are determined by the parameters χ_{12} and χ_{13}, the charge densities L_2 and L_3, and the combined effects of χ_{23} and L_2, of χ_{23} and L_3, and of L_2 and L_3. The term "combined effect" is used when the effect of varying two different parameters simultaneously is different from the isolated effects of varying the same parameters only one at the time. An example of such a combined effect is the $|\Delta\chi|$ effect discussed below.

The magnitudes and directions of change of L_2, L_3, and the combined effects are such that they all cancel out when L_2 and L_3 are equal. So for a fully charged system, the only effects left with significance are χ_{12} and χ_{13}. When L_2 and L_3 are different, however, this difference will have a dominant effect on the slope of the tie lines, which can be dampened somewhat by reduction of χ_{23}. In other words, χ_{23} then acquires an influence on the slopes, not just on the miscibility. Varying the molecular weights in the model experiments does not have any significant effect on the predicted tie-line slopes.

The miscibility of the system is determined by the χ_{23} parameter and by combined effects between χ_{12} and L_2, χ_{13} and L_3, M_2 and M_3, χ_{12} and L_3, χ_{13} and L_2, and L_2 and L_3. When L_2 and L_3 are equal, all the combined effects involving L_2 and L_3 cancel and only χ_{23} and the molecular weights have a significant influence on the predicted position of the coexistence curve. When the charge densities L_2 and L_3 are unequal, the combined effects become quite important and the system can actually be made less miscible by reducing the charge densities on one of the components, if the interaction parameter between this component and the solvent is altered by the component's loss of ionic nature.

Finding the Best Parameter Set. On the basis of the insights from the initial modeling, different values for the three parameters were tested by iterative modeling of the system in Figure 1a, where $M_2 = M_3 = 800$ (Table 1) and $L_2 = L_3 = 1$. When the fraction of charged monomers is reduced from unity, there exist two kinds of monomers on the chain, and they will not necessarily be described by the same values of the interaction parameters. By introducing a linear change

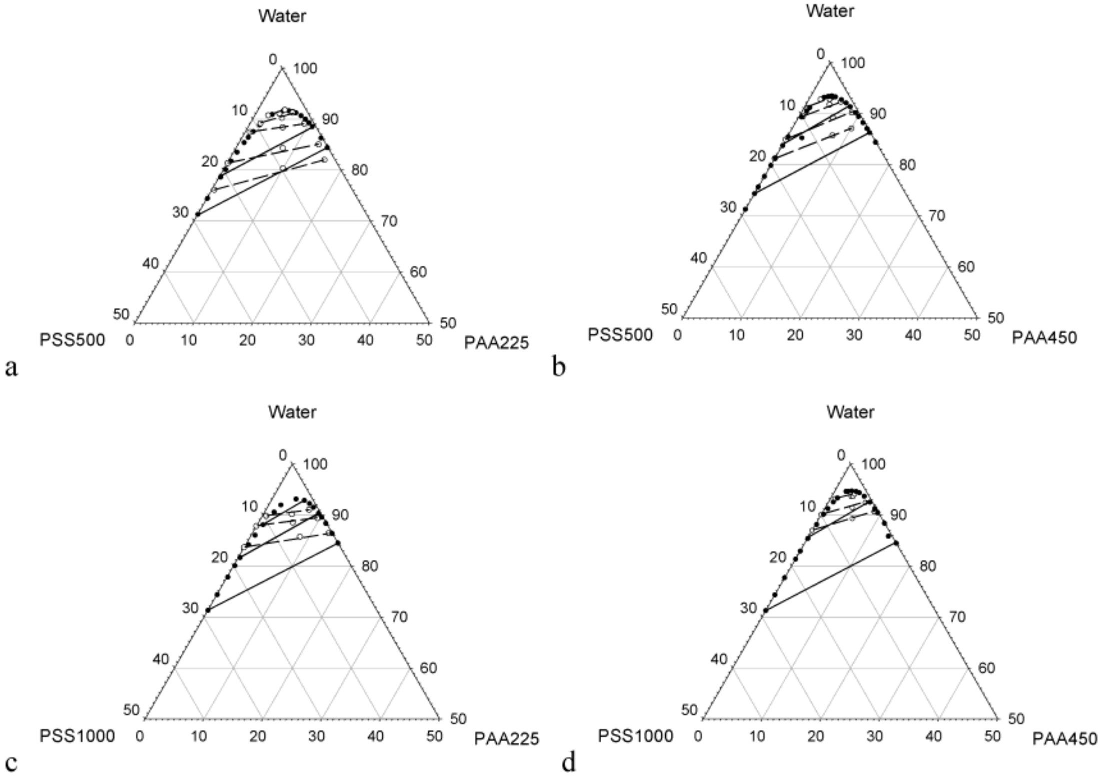

Figure 4. Phase diagrams comparing the experimental tie lines at 25 °C (open symbols, dashed lines) and the modeled tie lines (filled symbols, full lines) in water. Vertices are labeled with polymer type and molecular weights. Concentrations are in wt %. Model parameters for all systems are $\chi_{12} = 0.1$, $\chi_{13} = 0.1$, and $\chi_{23} = 0.21$, and degrees of polymerization are taken from Table 1. χ_{12} denotes the interactions between solvent and PSS monomers, χ_{13} denotes interactions between solvent and PAA monomers, and χ_{23} denotes interactions between monomers on the PSS and PAA chains.

when going from fully charged to reduced charge, this is assumed to include a weighted contribution from both types of monomers.

Because χ_{12} and χ_{13} were found not to influence the position of the coexistence curve, the strategy was to give these a value of zero and adjust χ_{23} until the predicted coexistence curve was in the right position. In this way, the value of χ_{23} was determined to be 0.21. The predicted tie-line slopes were approximately -0.5, while the experimental slope is -0.74.

Theoretically, it should be possible to adjust the slope through χ_{12} and χ_{13}, but in the model experiments these actually appear to have a negligible influence on the slope, when charge densities are equal. This is because the entropy of mixing of counterions dominates and the effect of the polymer−solvent interaction parameters has less impact on the predicted tie lines. For the fully charged systems in Figure 1, then, the parameters $\chi_{12} = \chi_{13} = 0$ and $\chi_{23} = 0.21$ would be satisfactory. Using other values for χ_{12} and χ_{13}, within a reasonable range, would be equally good, although this does not mean that they can be chosen entirely at random, as discussed above. The predicted coexistence curves for the systems in Figure 1, using the parameters $\chi_{12} = 0.1$, $\chi_{13} = 0.1$, and $\chi_{23} = 0.21$, are presented in Figure 4. They all correspond reasonably well to the experimental counterparts, apart from the tie-line slopes which were discussed above.

The next step was to model the systems with reduced charge density in Figure 2. Applying the parameters found above directly to the system in Figure 2c ($M_2 = 800$, $M_3 = 800$, $L_2 = 1$, $L_3 = 0.6$) did not result in a quantitative prediction of the coexistence curve.

If all the parameters are retained and only the charge density is varied, the model predicts that the system should be completely miscible before the charge density reaches $L_3 = 0.3$. From experiments, complete miscibility (for the observable region of the diagram) occurs when $L_3 = 0.2$. This is where the model does, in fact, predict that complete miscibility occurs (Figure 5a), if the χ parameters are allowed to vary linearly. This compares well with the experiments. The linear fit of parameter values is shown in Figure 5b.

The predicted coexistence curve with linearly adjusted χ parameters for the system PSS500−PAM200(60) (L_3 equals 0.6) is shown in Figure 6a ($\chi_{12} = 0.1$, $\chi_{13} = 0.26$, and $\chi_{23} = 0.17$). The predicted coexistence curve is placed somewhat too close to the solvent corner, and the predicted tie-line lengths are longer than observed in the experiments.

When the charge density is even lower, as in systems 4e and f, χ_{13} is further increased and χ_{23} is further reduced. Using the parameter set $\chi_{12} = 0.1$, $\chi_{13} = 0.38$, and $\chi_{23} = 0.14$, from Figure 5b, predicted the coexistence curve shown in Figure 6b. With these parameters, the observed reduction in miscibility for this system is not predicted. However, there are parameter sets that predict the coexistence curves for both these systems correctly, but it is not possible to predict them both correctly if the linear change requirement is adhered to, within a realistic range of parameter values. Large difference in the polymer−solvent interaction parameters, sometimes referred to as the $|\Delta\chi|$ effect,[8] tend to reduce miscibility. The reason for the predicted miscibility region that occurs above about 74% polymer in Figure 6b (not shown) is due to the fact that the polymer−polymer repulsions are too weak to cause

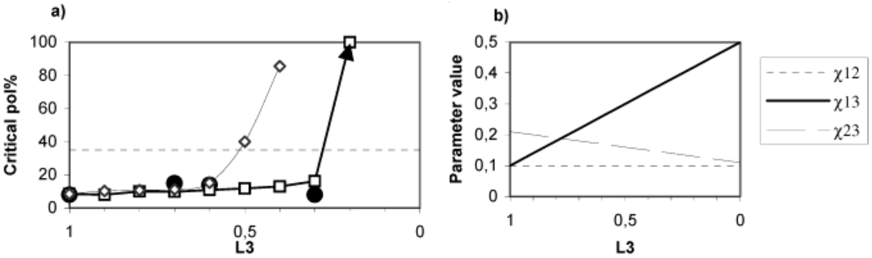

Figure 5. (a) Critical polymer concentrations are shown for predicted diagrams using the initial value of parameters for all values of L_3 (open diamonds) and using linearly changed values (open squares). Observed critical concentrations are also shown (filled circles). The dashed line is the approximate concentration limit for the experiments. (b) The corresponding values of the parameters χ_{12}, χ_{13}, and χ_{23}, changed linearly with charge density, L_3, on the PAM-τ chain.

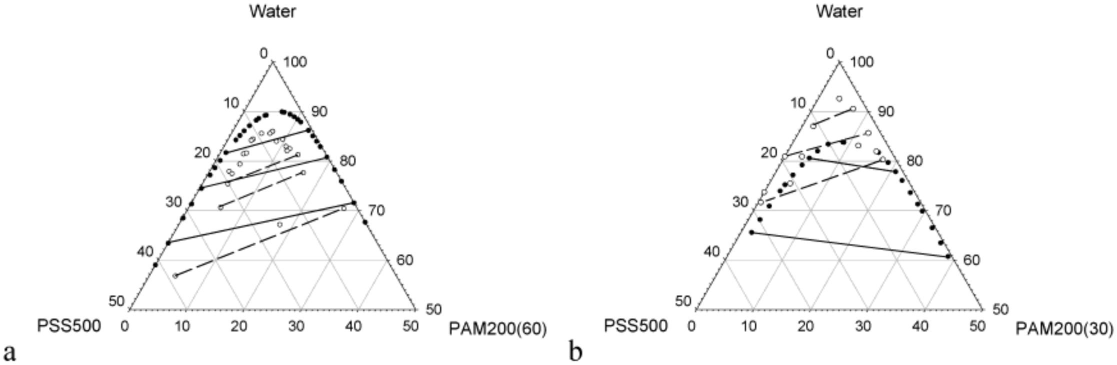

Figure 6. Phase diagrams comparing the experimental tie lines at 25 °C (open symbols, dashed lines) and the modeled tie lines (filled symbols, full lines) in water for the PSS500−PAM200(τ) systems when $\tau = 60\%$ (a) and 30% (b). Vertices are labeled with polymer type (charge density in parentheses). Concentrations are in wt %. Degrees of polymerization, $M_2 = M_3 = 800$. The model parameters used are $\chi_{12} = 0.1$, $\chi_{13} = 0.26$, $\chi_{23} = 0.17$ (a) and $\chi_{12} = 0.1$, $\chi_{13} = 0.38$, $\chi_{23} = 0.14$ (b).

segregation in this region without the added contribution from the $|\Delta\chi|$ effect. So increasing the χ_{13} parameter further relative to the χ_{12} parameter removes the predicted region of miscibility and moves the coexistence curve closer in line with the observed one, but that would not entail a linear change of χ_{13}. The predicted tie lines for the latter system (Figure 6b) slope in the opposite direction of the experimental lines. For $L_3 = 0.6$, they were also twisted in the same direction relative to the fully charged systems. This shows that the charge density has a much stronger influence on the tie-line slopes than the polymer−solvent interaction parameters. This is what was referred to above as the dominant effect of the counterion entropy of mixing over the pairwise interaction parameters.

The system PSS500−PAM200(20) is found not to demix even at high total polymer concentrations. Following the same linear change of the parameters ($\chi_{12} = 0.1$, $\chi_{13} = 0.42$, $\chi_{23} = 0.13$), this system was successfully predicted to be completely miscible, in accordance with experiments.

Conclusions

The phase behavior of a segregating mixture of two polyanions was investigated. It was observed that increased molecular weight decreases the miscibility of the components, which was interpreted in terms of the entropy of mixing. Higher ionic strength promotes segregation and tends to reduce the difference in polymer concentrations of the segregated phases.

When charge density is reduced on one of the polymeric components, the two-phase area is first slightly reduced, for 60% charge, and then slightly increased, for 30% charge, before complete miscibility is found at the lowest charge density studied (10−20%). Increasing the ionic strength, up to 1 M salt, in these systems does increase the two-phase area but does not raise the coexistence curve appreciably. The concentration difference between the separated phases is increased rather than reduced upon addition of salt, contrary to what is seen in the fully charged systems.

The experimental tie lines and coexistence curves have been compared to modeled tie lines. In the modeling, the interaction parameters χ_{13} and χ_{23} are varied in a linear manner as the charge density is reduced linearly from fully charged to low charge. The model presented is able to reconstruct the coexistence curve defined by the tie lines in a qualitative manner for most of the ternary systems presented. The major effect, that is, the onset of complete miscibility in the aqueous mixture of poly(styrenesulfonate) sodium salt and poly(acrylamide-*co*-acrylate) sodium salt, observed when the charge density on the latter is lower than 30%, is predicted.

Acknowledgment. We are grateful to the Norwegian Research Council for funding the work.

Appendix A. Computational Procedure for the Calculation of the Phase Diagrams

The procedure was originally developed by B. Jönsson (The thermodynamics of ionic amphipile−water systems, a theoretical analysis. Thesis, Lund, 1981) and has also been described by Åke Sjöberg (The mechanism of phase-separation in aqueous solutions of poly(ethylene glycol) and carbohydrates. Thesis, Lund, 1989).

There are four components (water, polymer 2, polymer 3, and counterions), but by the use of the electroneutrality condition this can be reduced to three by com-

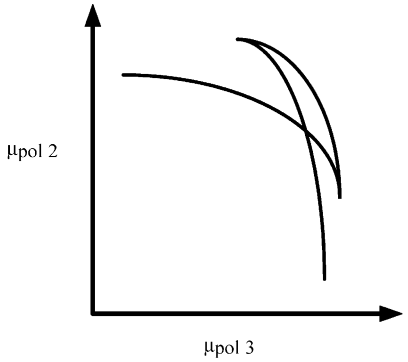

Figure 7. Chemical potential for component 2 versus component 3 at a fixed chemical potential for component 1. The point of self-intersection represents a two-phase equilibrium.

bining the polymer with its counterion to form an electroneutral pair. The three chemical potentials thus are

$$\mu_1 = f(\phi_{\mathrm{pol2}}, \phi_{\mathrm{pol3}}) \tag{A1}$$

$$\mu_{\mathrm{pol2}} = \mu_2 + L_2\mu_4 = g(\phi_{\mathrm{pol2}}, \phi_{\mathrm{pol3}}) \tag{A2}$$

$$\mu_{\mathrm{pol3}} = \mu_3 + L_3\mu_4 = h(\phi_{\mathrm{pol2}}, \phi_{\mathrm{pol3}}) \tag{A3}$$

(monovalent charges are assumed here for simplicity). The equations here are, for briefness, just presented as functions f, g, and h. A complete description is given in the theoretical section (eqs 3a–d). The chemical potentials are functions of the corresponding volume fractions, ϕ_1, ϕ_{pol2}, and ϕ_{pol3}. The sum of the volume fractions is unity, and the chemical potentials are therefore functions of two compositional variables.

The approach to calculate the phase equilibria is now to first select a value of the chemical potential of water, μ_1; the second step is to chose a value for the volume fraction of one of the polymers, for instance ϕ_{pol2}. From eq A1 it is now possible to numerically calculate ϕ_{pol3}. After this, all the other chemical potentials can be calculated. The procedure is now repeated for a new value of ϕ_{pol2}.

If the chosen value of the chemical potential of water corresponds to a two-phase situation, a plot of the chemical potentials, μ_{pol2} versus μ_{pol3}, will be as shown in Figure 7.

The line in Figure 7 will cross itself where two different compositions have the same chemical potential for all three components. By repeating the procedure for different chemical potentials of water, a phase diagram can easily be constructed. As a numerical convergence criterion it is required that the chemical potential for a component in the two phases should agree to within 10^{-6}, relative.

Appendix B. Tables of Polymeric and Ionic Compositions of Segregated Phases

Polymer compositions and charge balances in separated phases are shown in Tables 3–10. Values for PAA450 are converted from concentration of acid form to concentration of acrylate form, giving the same number of molecules in solution, to compare with PSS–PAA225 mixtures. The denotations top and bot refer to top and bottom phases, respectively.

References and Notes

(1) Albertsson, P. Å. *Partition of Cells, Particles and Macromolecules*, 3rd ed.; John Wiley: New York, 1986.
(2) Zaslavsky, B. Y. *Aqueous Two-Phase Partitioning*; Marcel Dekker: New York, 1995; (a) p 98, (b) p 116.
(3) Scott, R. *J. Chem. Phys.* **1949**, *17*, 3, 268–279.
(4) Scott, R. *J. Chem. Phys.* **1949**, *17* (3), 279–284.
(5) Tompa, H. *Polymer Solutions*; Butterworth: London, 1956.
(6) Flory, P. J. *Principles of Polymer Chemistry*; Cornell University Press: Ithaca, NY, 1953.
(7) Prigogine, I. *The Molecular Theory of Solution*; North-Holland: Amsterdam, 1967.
(8) Patterson, D. *Polym. Eng. Sci.* **1982**, *22* (2), 64–73.
(9) Khokhlov, A. R.; Nyrkova, I. A. *Macromolecules* **1992**, *25*, 1493.
(10) Piculell, L.; Bergfeldt, K.; Nilsson, S. In *Biopolymer Mixtures*; Mitchell, J., Hill, S., Harding, S., Eds.; Nottingham University Press: Nottingham, 1995; pp 13–35.
(11) Piculell, L.; Iliopoulos, I.; Linse, P.; Nilsson, S.; Turqois, T.; Viebe, C.; Zhang, W. In *Gums and stabilizers for the food industry*; Phillips, G. O., et al., Eds.; Oxford, 1994; Vol. 7.
(12) Gottschalk, M.; Linse, P.; Piculell, L. *Macromolecules* **1998**, *31*, 8407–8416.
(13) Lindvig, T.; Michelsen, M. L.; Kontogeorgis, G. M. *Fluid Phase Equilib.* **2002**, *203*, 247–260.
(14) Kouskoumvekaki, I. A.; Michelsen, M. L.; Kontogeorgis, G. M. *Fluid Phase Equilib.* **2002**, *202*, 325–335.
(15) Piculell, L.; Nilsson, S.; Falck, L.; Tjerneld, F. *Polym. Commun.* **1991**, *32*, 158.
(16) Bergfeldt, K.; Piculell, L.; Tjerneld, F. *Macromolecules* **1995**, *28*, 3360.
(17) Bergfeldt, K.; Piculell, L. J. *Phys. Chem.* **1996**, *14*, 5935.
(18) Perrau, M. B.; Iliopoulos, I. *Polymer* **1989**, *30*, 2112.
(19) Gupta, V.; Nath, S.; Chand, S. *Polymer* **2002**, *43*, 3387–3390.
(20) Thalberg, K.; Lindmann, B.; Bergfeldt, K. *Langmuir* **1991**, *7*, 2893–2898.
(21) Castelnovo, M.; Joanny, J.-F. *Eur. Phys. F. E* **2001**, *6*, 377–386.
(22) Mende, M.; Petzold, G.; Buchhammer, H.-M. *Colloid Polym. Sci.* **2002**, *280*, 342–351.
(23) Piculell, L.; Bergfeldt, K.; Gerdes, S. *J. Phys. Chem.* **1996**, *100*, 3675–3679.
(24) Katsunori Yoshida; Dubin, P. L. *Colloids Surf., A* **1999**, *147*, 161–167.
(25) Nilsson, S.; Blokhus, A. M.; Saure, A. *Langmuir* **1998**, *14*, 6082–6085.
(26) Yamaguchi, Y.; Inaba, Y.; Uchiyama, H.; Kunieda, H. *Colloid Polym.* **1999**, *277*, 1117–1124.
(27) Hansson, P.; Schneider, S.; Lindman, B. *J. Phys. Chem. B* **2002**, *106*, 9777–9793.
(28) Piculell, L.; Lindman, B. *Adv. Colloid Interface Sci.* **1992**, *41*, 149–178.
(29) Iliopoulos, I.; Frugier, D.; Audebert, R. *Polym. Prepr.* **1989**, *30* (2), 371–372.
(30) Roland, C. M. *Macromolecules* **1987**, *20* (10), 2557–2563.
(31) Cesarano, J., III; Aksay, I. A.; Bleier, A. *J. Am. Ceram. Soc.* **1988**, *71* (4), 250–255.
(32) Gunari, A. A.; Gundiah, S. *Makromol. Chem.* **1981**, *182*, 1–8.
(33) Geladi, P.; Kowalski, B. R. *Anal. Chim. Acta* **1986**, *185*, 1–17.
(34) Kolthoff, I. M.; Sandell, E. B.; Meehan, E. J.; Bruckenstein, S. *Quantitative Chemical Analysis*, 4th ed.; The Macmillan Co.: Toronto, 1969; p 813.
(35) Richards, E. G. *An introduction to the physical properties of large molecules in solution*; Cambridge University Press: Cambridge, 1980.
(36) Einaga, Y. *Prog. Polym. Sci.* **1994**, *19*, 1–28.

MA021442T